NASA TN D-1289

TECHNICAL NOTE

D-1289

ABSORPTION AND EMISSION CHARACTERISTICS

OF DIFFUSE SPHERICAL ENCLOSURES

By E. M. Sparrow and V. K. Jonsson

University of Minnesota,
Minneapolis, Minnesota

NATIONAL AERONAUTICS AND SPACE ADMINISTRATION

WASHINGTON June 1962

1G

E-1622

NATIONAL AERONAUTICS AND SPACE ADMINISTRATION

TECHNICAL NOTE D-1289

ABSORPTION AND EMISSION CHARACTERISTICS OF DIFFUSE SPHERICAL ENCLOSURES

By E. M. Sparrow and V. K. Jonsson

SUMMARY

An analysis was made to determine the energy absorbed when radiation from an external source enters a spherical cavity with diffusely reflecting walls. It was found that both the overall energy absorbed in the cavity and the local distribution of absorbed energy could be expressed in terms of simple algebraic equations that are valid for any arbitrary spatial and directional distribution of the incoming radiation. In addition, the characteristics of an isothermal spherical cavity as a possible source of near black-body radiation were investigated. This information was also expressed by simple algebraic relations.

INTRODUCTION

The thermal radiation characteristics of spherical cavities are of practical importance in connection with the absorption of radiant energy for both outer-space and terrestrial applications. For example, a study of the relative merits of various absorber configurations for a space-vehicle solar power system has shown the spherical cavity to be quite attractive (ref. 1). In addition, spherical cavities are of potential use as emitters of black-body radiation.

An analysis, described herein, was made to determine both the absorption and emission characteristics of spherical cavities, the surfaces of which are diffuse reflectors and emitters (i.e., Lambert's cosine law is obeyed). The absorption analysis sought to provide the following information: Given the amount of radiant energy entering the cavity, what fraction is ultimately absorbed within the cavity. It is shown that this overall absorption result can be derived without approximation in terms of a simple closed-form expression that is valid for any arbitrary spatial and directional distribution of the incoming radiation. A second aim of the absorption analysis was to provide the local distribution of absorbed energy as a function of surface location within the cavity.

This local absorption information is also derived in terms of a simple closed-form algebraic equation valid for any arbitrary distribution of incoming radiation. These general properties of the spherical cavity appear not to have been reported by previous investigators.

The absorption problem is treated herein without recourse to the emission problem. What was being sought was an effective (or apparent) absorptivity that characterizes the combined behavior of the cavity geometry and its surface absorptivity. This effective absorptivity for the cavity may be considered a property in the same sense as is the surface absorptivity a property of a plane surface. The reemission of radiant energy depends upon the particular thermal boundary condition that is prescribed at the surface of the cavity (e.g., isothermal, adiabatic, or uniform heat flux). The results derived herein for the local distribution of absorbed energy can be used as input data for solving the reemission problem for any arbitrarily prescribed thermal boundary condition. Thus, the results of this report are meant to have general applicability extending beyond particular thermal boundary conditions. The present analysis utilizes a temperature-independent surface absorptivity that is defined as the fraction of the incoming energy absorbed over the entire range of wavelengths. The gray-body assumption need not be made. The results can equally well be used on a monochromatic basis and then integrated over all wavelengths.

The second part of this report is concerned with the emission characteristics of isothermal spherical cavities. This study is motivated by the possible utilization of such cavities as sources of black-body energy. In such applications, care would be taken to ensure that the energy level of any external radiation entering the cavity would be much lower than the energy level of radiation emitted within the cavity. With this in mind, external radiation is not included in the cavity-emission analysis.

This research was sponsored by the National Aeronautics and Space Administration through the Office of Grants and Research Contracts.

SYMBOLS

A surface area

A^* surface area of cavity interior

B radiosity: radiant flux leaving surface element per unit time and area

E-1022

e_d	rate of energy carried by incoming diffuse stream per unit area of cavity opening
e_r	rate of energy carried by incoming parallel ray bundle per unit area normal to ray
F	angle factor
H	incident energy per unit time and area
Q	overall rate of energy absorption
Q'	overall rate of energy streaming from cavity
q	local rate of energy absorption per unit area
q'	local rate of heat loss per unit area
R	radius of sphere
r	distance (fig. 2)
S	rate of incoming radiation
s	distribution of incoming radiation per unit surface area
T	absolute temperature
x,y,z	coordinates
α	surface absorptivity
α_a	apparent absorptivity
β	inclination angle of rays
ϵ	emissivity
ϵ_a	apparent emissivity
θ,φ	coordinate angles
φ^*	opening angle of cavity
σ	Stefan-Boltzmann constant

ANGLE FACTOR FOR DIFFUSE INTERCHANGE

As a basis for the analysis that follows, the angle factor for diffuse interchange within a spherical cavity must be known. The angle factor is the fraction of the radiant energy leaving one surface element that is incident on some other surface element. The derivation of the angle factor for two elements located on a spherical shell is based on sketch (a). For radiant interchange between two diffuse infinitesimal

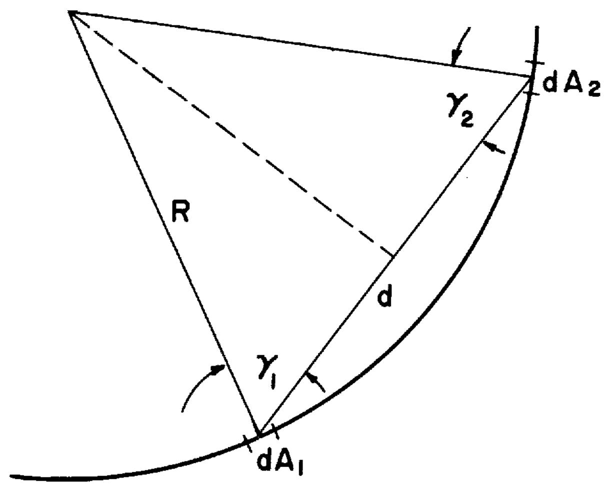

(a)

surface elements, the angle factor takes the following form (e.g., ref. 2):

$$dF_{1-2} = \frac{\cos \gamma_1 \cos \gamma_1}{\pi d^2} dA_2 \tag{1}$$

Written in this way, the angle factor represents the fraction of the radiant energy leaving dA_1 that reaches dA_2. The distance as measured along the connecting line between dA_1 and dA_2 is denoted by d. The angles γ_1 and γ_2 are, respectively, formed by the normals to dA_1 and dA_2 and the connecting line between the elements. From sketch (a) it is easily seen that

$$\cos \gamma_1 = \cos \gamma_2 = \frac{(d/2)}{R}$$

E-1622

With this, equation (1) becomes

$$dF_{1-2} = \frac{dA_2}{4\pi R^2} \tag{2a}$$

The remarkable aspect of this result is that the angle factor is independent of the orientation and the position of the elements. This is a unique property of the spherical cavity. With cognizance of this property taken, equation (2a) can be generalized to read

$$F_{1-2} = \frac{A_2}{4\pi R^2} \tag{2b}$$

where the surface elements 1 and 2 may be either finite or infinitesimal.

The findings of the previous paragraph easily show that radiation which is diffusely emitted or reflected from a surface element will reach every unit area of the spherical cavity in uniform amount. Thus, if A^* is the surface area of the cavity interior, the fraction $A^*/4\pi R^2$ of the energy leaving an element will fall upon the surfaces of the cavity and another fraction $1 - (A^*/4\pi R^2)$ will escape through the opening.

ABSORPTION CHARACTERISTICS

Overall Energy Absorption

Consider radiation from an external source streaming into a spherical enclosure, which is diagrammed in sketch (b). The radius of the

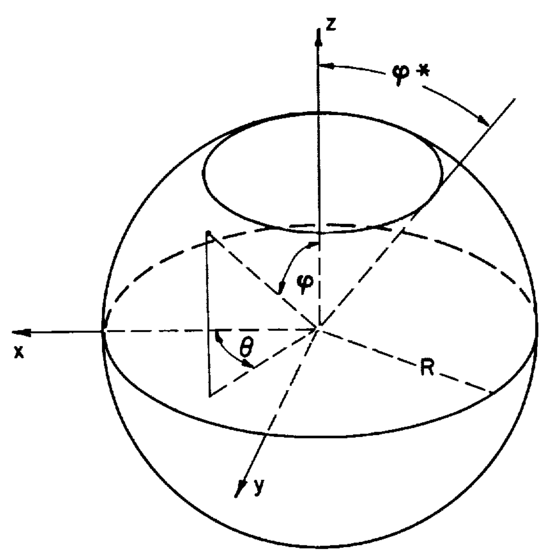

(b)

sphere is R, and the angle φ^* defines the opening of the cavity. The angles φ and θ are, respectively, the polar and plane angles in a standard set of spherical coordinates. The corresponding surface area A^* of the cavity interior is

$$A^* = 2\pi R^2(1 + \cos \varphi^*) \tag{3}$$

The spatial and directional distribution of the incoming radiation may be completely arbitrary, and the rate of incoming energy is denoted by S (e.g., Btu/hr).

E-1622

Consideration of the incoming energy shows that upon first contact with the surface an amount

$$Q_1 = \alpha S \tag{4a}$$

is absorbed, and $(1 - \alpha)S$ is reflected in all directions. Of this reflected energy, it follows, from the foregoing discussion of angle factors, that an amount $(1 - \alpha)S \dfrac{A^*}{4\pi R^2}$ remains within the cavity and is uniformly distributed over the surface. Of the reflected energy thus incident on the surface, a fraction α is absorbed, that is,

$$Q_2 = \alpha S\left[(1 - \alpha) \frac{A^*}{4\pi R^2}\right] \tag{4b}$$

and another fraction $(1 - \alpha) \dfrac{A^*}{4\pi R^2}$ is re-reflected and then returns to the surface. Once again, a fraction α is absorbed, that is,

$$Q_3 = \alpha S\left[(1 - \alpha) \frac{A^*}{4\pi R^2}\right]^2 \tag{4c}$$

and another fraction $(1 - \alpha) \dfrac{A^*}{4\pi R^2}$ reflects and returns to the surface. If account were kept of all the successive absorptions Q_i, the total energy absorbed Q could be determined by simply summing the separate contributions as given by equations (4a), (4b), (4c), and so forth:

$$Q = \sum_{i=1}^{\infty} Q_i = \alpha S\left\{1 + (1 - \alpha) \frac{A^*}{4\pi R^2} + \left[(1 - \alpha) \frac{A^*}{4\pi R^2}\right]^2 + \ldots\right\} \tag{5}$$

The series within the braces is a geometric progression and therefore can be summed in closed form. Making use of this sum and introducing A^* from equation (3) gives

$$Q = \frac{\alpha S}{1 - 0.5(1 - \alpha)(1 + \cos \varphi^*)} \tag{6}$$

E-1622

As a convenient representation of the overall absorption results, there is introduced the apparent absorptivity, which is defined as

$$\alpha_a = \frac{\text{Total energy absorbed}}{\text{Total incoming energy}} = \frac{Q}{S} \tag{7}$$

Substituting for Q from equation (6) yields the expression for α_a as

$$\alpha_a = \frac{\alpha}{1 - 0.5(1 - \alpha)(1 + \cos \varphi^*)} \tag{8}$$

The remarkable conclusion, which follows from this, is that the apparent absorptivity is independent of the detailed manner in which the incoming energy enters the enclosure; therefore, equation (8) applies in general. The only parameters are the opening angle φ^* and the surface absorptivity α.

The apparent absorptivity, as given by equation (8), is plotted in figure 1 as a function of φ^* for parametric values of α. Inspection of the figure reveals that the apparent absorptivity of the cavity always exceeds the surface absorptivity α. This finding is related to the additional opportunities for absorption that accompany the multi-reflections within the cavity (the so-called "cavity effect"). The increase of α_a relative to α is greatest for surfaces of low absorptivity and for cavities with small openings (i.e., small φ^*). Even for a moderately large opening angle such as 60°, however, there is already a substantial deviation between α_a and α. For very small values of φ^*, the apparent absorptivity is very close to unity regardless of the actual surface absorptivity.

Local Energy Absorption

Thus far consideration has been given to the absorption characteristics of the enclosure as a whole. Now, attention will be directed to the energy absorbed locally at various positions on the cavity wall. The distribution of the incoming energy over the interior of the cavity is represented by $s(\varphi,\theta)$ per unit surface area (e.g., Btu/(hr)(sq ft). The relation between the local distribution s and the total rate of incoming energy S is given by

$$S = \int_{\theta=0}^{2\pi} \int_{\varphi=0}^{\pi} s(\varphi,\theta) R^2 \sin \varphi \, d\theta \, d\varphi \tag{9}$$

The radiant energy locally absorbed per unit time and area is denoted by q.

From the first contact of the incoming radiation with the surface, the energy locally absorbed per unit time and area is

$$q_1 = \alpha s \tag{10a}$$

All subsequent absorptions of reflected and re-reflected radiation, however, take place uniformly at all locations in the enclosure. From all absorptions following the first contact, therefore, the energy locally absorbed per unit area is most simply obtained by subtracting αS from Q (eq. (6)) and then dividing by the surface area A^*. From this it follows that

$$q - q_1 = \frac{\alpha(1 - \alpha)(S/4\pi R^2)}{1 - 0.5(1 - \alpha)(1 + \cos \varphi^*)} \tag{10b}$$

Then, q is obtained by combining equations (10a) and (10b):

$$q = \alpha s + \frac{\alpha(1 - \alpha)(S/4\pi R^2)}{1 - 0.5(1 - \alpha)(1 + \cos \varphi^*)} \tag{11}$$

Equation (11) applies for any arbitrary surface distribution of incoming radiation. The final explicit result for q is obtained by introducing the particular distribution function $s(\varphi,\theta)$ that may be of interest.

Contrasting the simplicity of the local absorption result that has just been derived with what would be found for nonspherical configurations is interesting. In general, for other cavity shapes, solving an integral equation to determine q would be necessary and, almost always, numerical means would be required. In many situations, such solutions would have to be carried out separately for each distribution function s of interest. When cognizance of this is taken, the simplicity and generality of equation (11) is clearly evident.

Applications of General Analysis

To illustrate the use of the foregoing analysis, application will be made to two important limiting cases. The first is concerned with incoming radiation traveling in a bundle of parallel rays, while the second treats incoming radiation that is diffusely distributed over the opening of the cavity.

Parallel rays. - Consider radiation arriving in a parallel-ray bundle as illustrated in figure 2. The rays travel in the direction of the positive x-axis and make an angle β with the vertical. The energy carried by the ray bundle may be characterized by e_r per unit area normal to the ray (e.g., Btu/(hr)(sq ft)). An obvious example would be the solar constant. Because the area of a surface tightly stretched across the opening of the spherical cavity is $\pi(R \sin \varphi^*)^2$ and the projection of the rays along the normal to this surface is accomplished by $\cos \beta$, the total energy S entering the enclosure is

$$S = e_r \pi R^2 \cos \beta \sin^2 \varphi^* \qquad (12)$$

The overall rate of energy absorption in the cavity is $\alpha_a S$, where α_a may be calculated from equation (8) or read from figure 1.

Next, the surface distribution of the incoming energy $s(\varphi, \theta)$ may be determined. Depending on the inclination angle β and the opening angle φ^*, the incoming rays may be directly incident on only part of the surface; the remaining portion receives radiant energy because of internal reflections alone. The portion that is directly irradiated may be called the no-shadow region, while the portion receiving only reflected energy may be called the shadow region. In the no-shadow region, the distribution function s (which is per unit surface area) may be derived by projecting the incoming rays along the surface normal. Writing expressions for unit vectors lying along the local surface normal (i.e., the radius vector) and along the incoming rays and then taking the scalar product shows that

$$s = e_r(\cos \theta \sin \varphi \sin \beta - \cos \varphi \cos \beta) \qquad (13a)$$

in the no-shadow region. In the shadow region,

$$s = 0 \qquad (13b)$$

These expressions for s, along with equation (12) for S, may be utilized in determining the local distribution of the absorbed energy as given by equation (11).

In order to render equations (13) fully useful, the boundary between the shadow and no-shadow regions must be determined. To illustrate the method of analysis, consider the case where $\varphi^* > 90^\circ$, that is, a spherical shell smaller than a hemisphere as pictured in figure 2. When the inclination angle $\beta < (\varphi^* - 90^\circ)$, the incoming radiation will fall directly on all parts of the surface (albeit nonuniformly). When $\beta > (\varphi^* - 90^\circ)$, a shadow region coexits along with a region of direct illumination. The coordinates of the boundary curve between the shadow and no-shadow regions will be found with the aid of figure 2. The upper part of the figure is a plan view of the spherical shell showing radiation arriving from the right. The lower part of the figure is an elevation view cut through the spherical shell at a typical location $y =$ constant. In the lower part of figure 2, there is shown a limiting ray that grazes the rim of the shell and strikes the surface at a location x, z; this is the boundary point between the shadow and no-shadow regions. From the geometry of the figure

$$x = -r\cos(2\beta - \xi), \qquad z = -r\sin(2\beta - \xi) \tag{14a}$$

Also, it is easy to show that

$$r\sin\xi = -R\cos\varphi^*, \qquad r\cos\xi = \sqrt{R^2\sin^2\varphi^* - y^2} \tag{14b}$$

The distance r and angle ξ can be eliminated by combining equations (14a) and (14b), and this yields

$$\left.\begin{aligned} x &= R\cos\varphi^*\sin 2\beta - \sqrt{R^2\sin^2\varphi^* - y^2}\cos 2\beta \\ z &= -\sqrt{R^2\sin^2\varphi^* - y^2}\sin 2\beta - R\cos\varphi^*\cos 2\beta \end{aligned}\right\} \tag{15}$$

Equations (15) constitute a parametric representation of the boundary curve between the shadow and no-shadow regions.

When $\varphi^* < 90^\circ$ (spherical shell larger than a hemisphere), the boundary curve is also defined by limiting rays that graze the rim of the cavity opening and intersect the shell. As illustrated on figure 3, however, rays that graze at all points around the rim must be considered. From the rays that graze at the forward edge of the rim (toward the incoming rays), the x, z-coordinates of the shadow, no-shadow boundary remain as given by equations (15). From the rays that graze at the rearward edge of the rim, the boundary curve is found to be

$$\left.\begin{aligned} x &= R\cos\varphi^*\sin 2\beta + \sqrt{R^2\sin^2\varphi^* - y^2}\cos 2\beta \\ z &= \sqrt{R^2\sin^2\varphi^* - y^2}\sin 2\beta - R\cos\varphi^*\cos 2\beta \end{aligned}\right\} \tag{16}$$

To provide some feeling for the nature of the boundary curve, it is useful to project it into the x, z- and x, y-planes. The projections have the following equations:

$$\left.\begin{aligned} x\sin 2\beta - z\cos 2\beta &= R\cos\varphi^* \\ \frac{(x - R\cos\varphi^*\sin 2\beta)^2}{R^2\sin^2\varphi^*\cos^2 2\beta} + \frac{y^2}{R^2\sin^2\varphi^*} &= 1 \end{aligned}\right\} \tag{17}$$

These projections are, respectively, a straight line and an ellipse. This indicates that the boundary curve cuts out a circle or a part of a circle on the surface of the spherical shell.

E-1622

To illustrate these results, figure 4 has been prepared to show the projections of the boundary curve in plan and elevation views (x,y- and x,z-planes, respectively). The left side of the figure corresponds to an enclosure where $\varphi^* > 90^\circ$. Projections are shown for inclination angles $\beta < 45^\circ$, $= 45^\circ$, and $> 45^\circ$. The right side corresponds to $\varphi^* < 90^\circ$, and projections are shown for $\beta < 45^\circ$ and $\beta = 45^\circ$. The case of $\beta > 45^\circ$ was not included in order to preserve clarity of the figure.

E-1622

Diffuse incoming radiation. - Diffuse radiant energy is considered uniformly distributed over the opening of the spherical cavity. The energy carried by the diffuse stream may be characterized by e_d per unit area of the cavity opening. For purposes of analysis and without loss of generality, this energy may be regarded as coming from a black, isothermal spherical cap of spherical radius R and emissive power e_d, which fits over the opening of the cavity. This arrangement is pictorially illustrated in sketch (c). Such a spherical cap gives rise to a

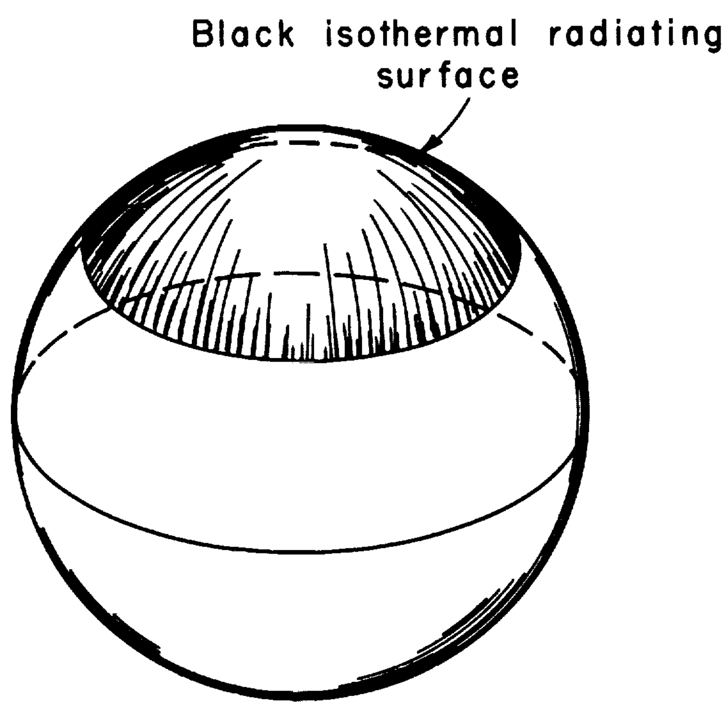

(c)

diffuse stream of radiation, uniformly distributed across the cavity opening. Since a black surface is a diffuse emitter, radiant energy coming from the spherical cap is uniformly distributed along the walls of the cavity (see discussion following eq. (2b)). This same statement also applies to any stream of incoming diffuse energy uniformly distributed across the cavity opening.

The opening of the spherical cavity has an area $\pi(R \sin \varphi^*)^2$ and, therefore, the rate S at which radiant energy enters the cavity is

$$S = e_d \pi R^2 \sin^2\varphi^* \tag{18}$$

A fraction α_a of this energy quantity is absorbed within the cavity. Since the incoming radiation is uniformly distributed over the walls of the cavity (area A^*), the distribution function s is independent of position and is equal to

E-1622

$$s = \frac{S}{A^*} = \frac{0.5 e_d \sin^2\varphi^*}{1 + \cos \varphi^*} \tag{19}$$

Introducing these expressions into equation (11) gives the following result for the local rate of energy absorption q:

$$q = e_d \frac{0.5 \alpha \sin^2\varphi^*/(1 + \cos \varphi^*)}{1 - 0.5(1 - \alpha)(1 + \cos \varphi^*)} \tag{20}$$

Inspection of equation (20) reveals that q is uniform along the walls of the cavity. This result may be contrasted with the findings for the case of the parallel ray bundle, for which q is a function of position for any inclination angle of the rays.

EMISSION CHARACTERISTICS

Consideration is now given to the emission characteristics of a diffuse, isothermal, spherical cavity (temperature T). Radiation entering the cavity from an external source is not included in the analysis for reasons already discussed in the INTRODUCTION. The surface absorptivity and emissivity relate, respectively, to energy absorption and emission over the entire wavelength range. The gray-body assumption is not required, so that α need not be equal to ϵ. The analysis as given in the following paragraphs can also be carried out on a monochromatic basis.

The starting point of the analysis is a radiant flux balance on a typical element of surface. The energy leaving the surface element per unit time and area is equal to the sum of the emitted energy plus the reflected portion of the incident energy. The leaving energy per time and area is denoted by B and is called the radiosity; while, the incident energy per unit time and area is denoted by H. With these, the radiant flux balance becomes

$$B(\varphi_o, \theta_o) = \epsilon\sigma T^4 + (1 - \alpha) H(\varphi_o, \theta_o) \tag{21}$$

E-1622

where φ_o, θ_o are the coordinates of a particular surface location and the reflectivity has been replaced by $(1 - \alpha)$. In reference 3, it is shown that the radiant flux incident at any given point is obtained by taking the radiant energy leaving another location, multiplying by an appropriate angle factor, and then integrating over the entire surface:

$$H(\varphi_o, \theta_o) = \int_{A^*} B(\varphi, \theta) dF \tag{22}$$

Since both the temperature and the angle factor are uniform throughout the cavity, it is easily seen that the radiosity B will also be independent of position; therefore,

$$H = B \int_{A^*} dF = \frac{BA^*}{4\pi R^2} \tag{23}$$

Introducing equation (23) into (21) and solving for B gives

$$\frac{B}{\sigma T^4} = \frac{\epsilon}{1 - 0.5(1 - \alpha)(1 + \cos \varphi^*)} \tag{24}$$

in which A^* has been evaluated from equation (3).

If the cavity is to be used as a black-body energy source, $B/\sigma T^4$ is a measure of its effectiveness. Clearly, it would be desired that $B/\sigma T^4$ approach as closely as possible to unity. If $\alpha \approx \epsilon$ (gray body), $B/\sigma T^4$ can be read directly from figure 1. The figure reveals that a spherical enclosure with a small hole (small φ^*) is a very effective black body. If $\alpha \neq \epsilon$, figure 1 may still be used, but the values read from the ordinate must be multiplied by ϵ/α.

The net local heat flux q' per unit area is the difference between the radiant flux leaving the surface element and the flux that is incident on it:

$$q' = B - H \tag{25}$$

Substituting equations (23) and (24) for H and B, respectively, and rearranging yields

$$q' = \epsilon\sigma T^4 \frac{0.5 \sin^2\varphi^*/(1 + \cos \varphi^*)}{1 - 0.5(1 - \alpha)(1 + \cos \varphi^*)} \tag{26}$$

Inspection of this equation reveals that q' is uniform over the surface. It is also interesting to note that q' represents the rate at which energy must be locally supplied to the wall of the spherical shell in order to maintain the isothermal condition.

The overall rate Q' at which radiant energy streams outward from the opening of the cavity may be calculated by multiplying equation (26) by A^*. A convenient representation of this overall heat-transfer result may be made in terms of an apparent emissivity ϵ_a, defined as follows:

$$\epsilon_a = Q'/Q'_{bb} \tag{27}$$

where Q'_{bb} is the radiant energy streaming from a black-walled isothermal cavity. The energy loss from a black cavity is precisely equal to the radiation from a black isothermal disk stretched over the cavity opening

$$Q'_{bb} = \sigma T^4 \pi R^2 \sin^2\varphi^* \tag{28}$$

Then, multiplying equation (26) by A^* and dividing by Q'_{bb}, gives

$$\epsilon_a = \frac{\epsilon}{1 - 0.5(1 - \alpha)(1 + \cos\varphi^*)} \tag{29}$$

Comparison of this result with equation (8) reveals that $\epsilon_a = \alpha_a$ for a gray-walled cavity. For this condition, ϵ_a may be read directly from figure 1. If $\alpha \neq \epsilon$, the ordinates are to be multiplied by ϵ/α.

Inspection of figure 1 suggests that the spherical cavity is an attractive configuration for potential application as a source of nearly black-body radiation.

CONCLUDING REMARKS

The foregoing analysis demonstrated a unique property of the diffuse spherical cavity, namely, that the absorption and emission characteristics can be represented in terms of simple, closed-form algebraic equations. In general, for nonspherical configurations, solving integral equations would be necessary to obtain corresponding information. In almost all instances, numerical techniques would have to be employed in conjunction with a digital computer.

E-1622

Because of its simplicity, the local absorption relation (eq. (11)) is in an especially convenient form to serve as input data for analyses involving reemission and perhaps energy storage. Considerations relating to energy storage arise in systems that may not be irradiated continuously and that employ fluids or salt solutions as heat reservoirs. Although such analyses may involve transient conditions, the applicability of equation (11) is not altered.

One situation occurs in which the simultaneous problem of incoming external radiation and surface emission can be solved by a simple linear combination of the results for the separate absorption and emission problems. This is the case of the isothermal surface. The net overall heat loss is given by the difference $Q' - Q$ (Q' is overall rate of energy streaming from cavity and Q is overall rate of energy absorption), while the net local heat loss is found from $q' - q$ (q' is net local rate of heat loss per unit area and q is local rate of energy absorption per unit area).

Heat Transfer Laboratory
Department of Mechanical Engineering
University of Minnesota
Minneapolis, Minn.
February 28, 1962

REFERENCES

1. Stephens, Charles W., and Haire, Alan M.: Internal Design Consideration for Cavity-Type Solar Absorbers. ARS Jour., vol. 31, no. 7, July 1961, pp. 896-901.

2. Eckert, E. R. G., and Drake, R. M., Jr.: Heat and Mass Transfer. McGraw-Hill Book Co., Inc., 1959, p. 396.

3. Sparrow, E. M., Gregg, J. L., Szel, J. V., and Manos, P.: Analysis, Results, and Interpretation for Radiation Between Some Simply-Arranged Gray Surfaces. Jour. Heat Transfer, ser. C, vol. 83, no. 2, May 1961, pp. 207-214.

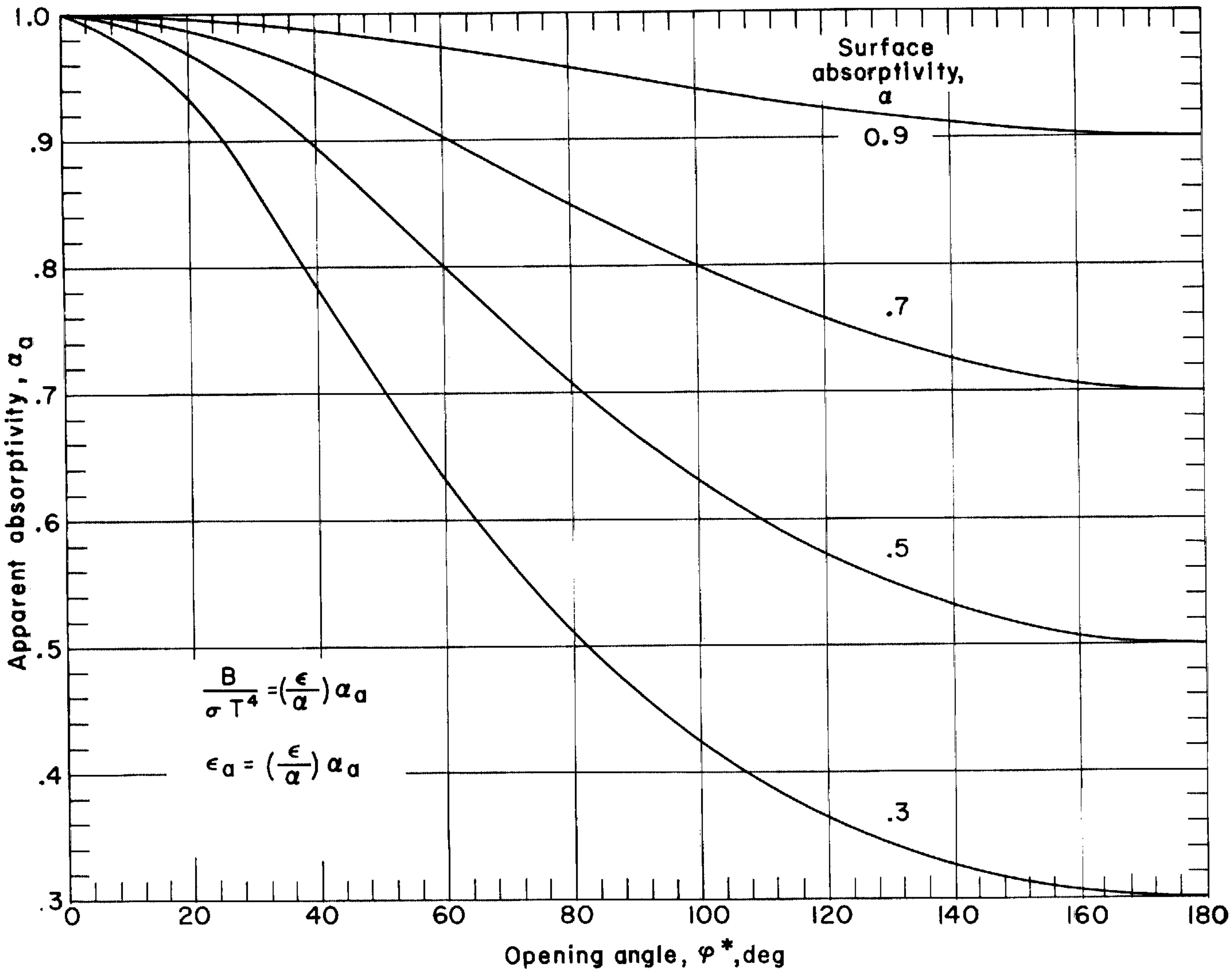

Figure 1. - Absorption and emission characteristics of spherical cavity.

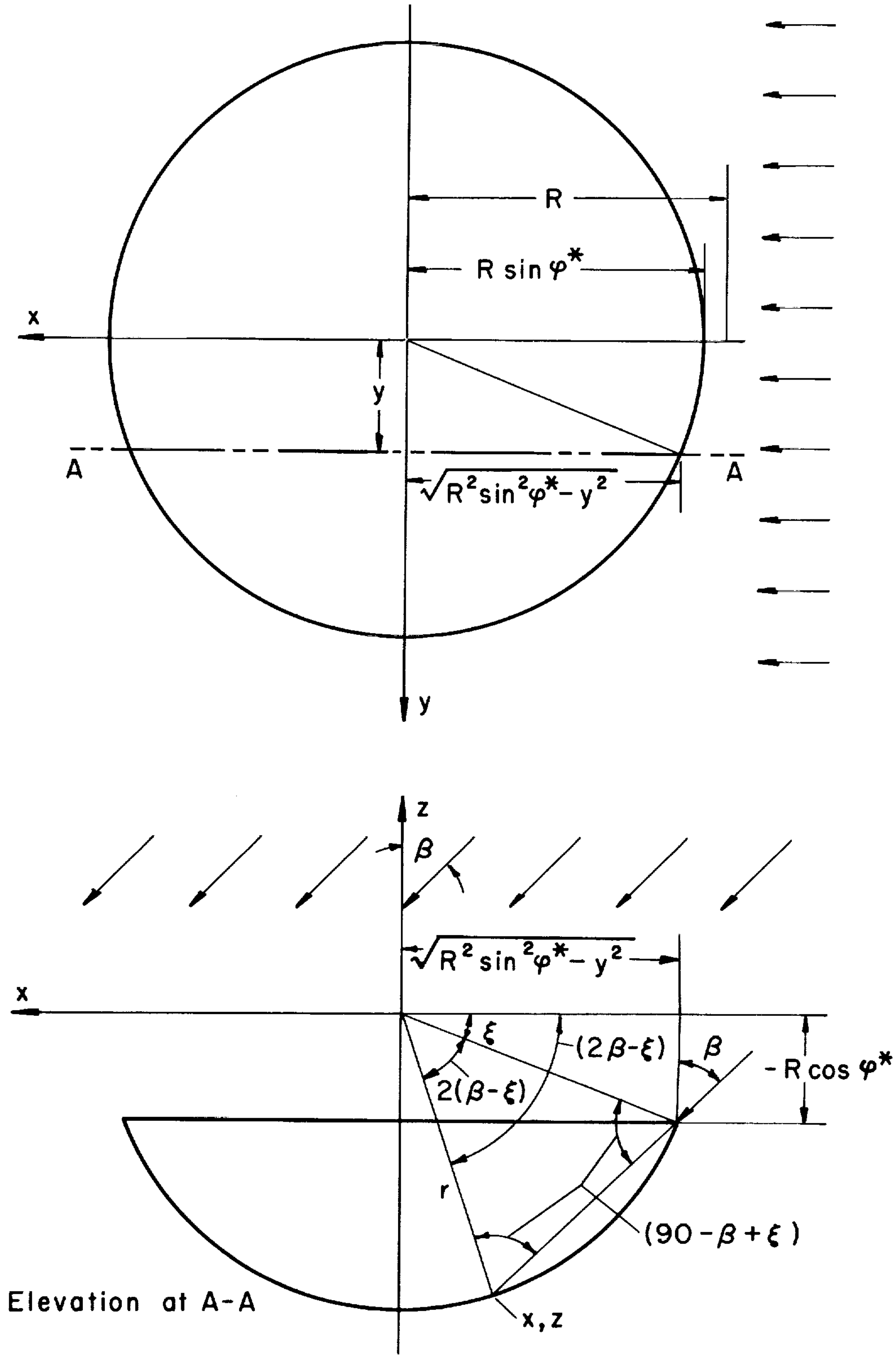

Figure 2. - Diagram for determining boundary between shadow and no-shadow regions; spherical cavity with opening angle of cavity $\varphi^* > 90^\circ$.

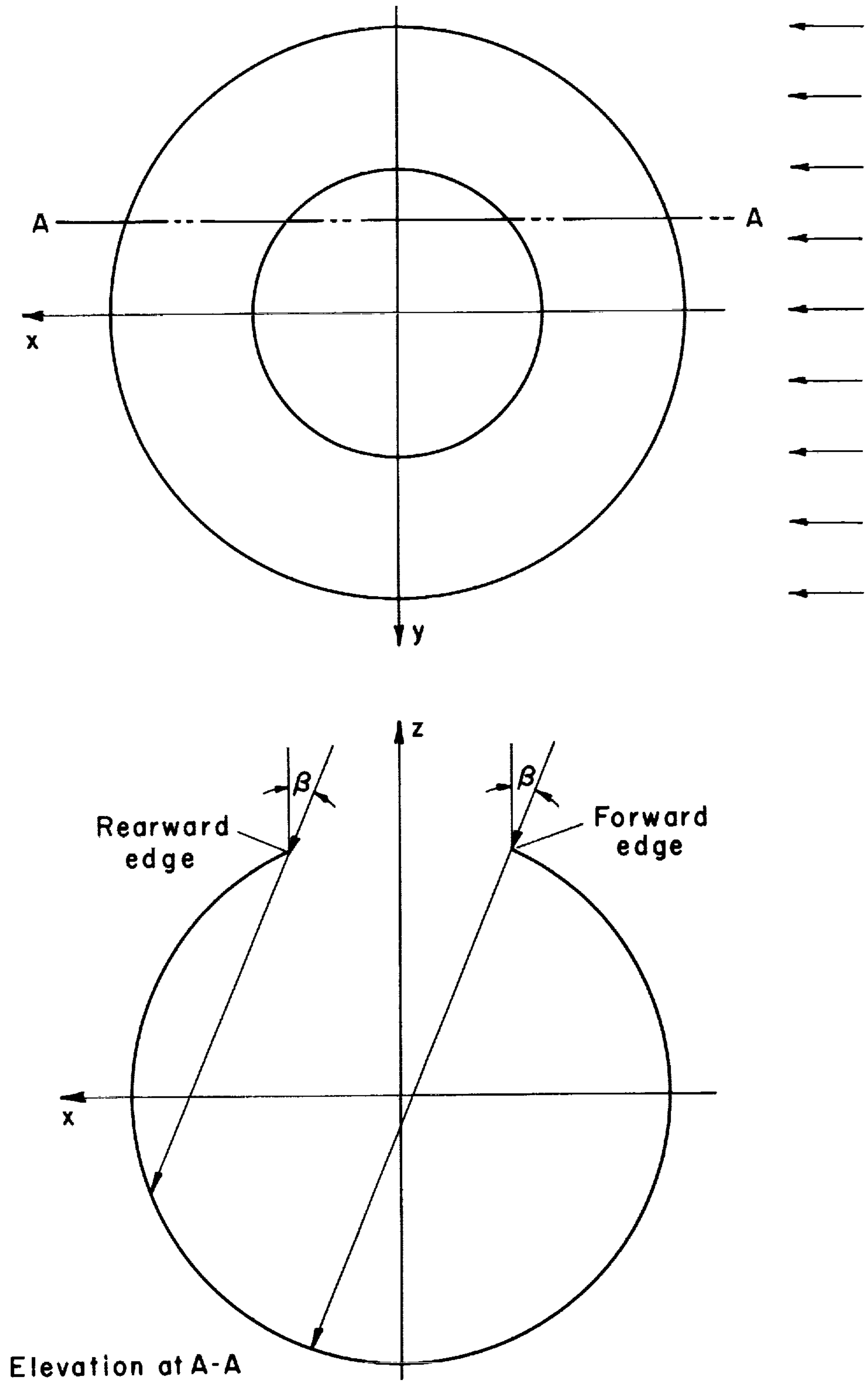

Figure 3. - Shadow, no-shadow boundary determined by rays grazing at forward and rearward edge of rim; spherical cavity with opening angle of cavity $\varphi^* < 90^\circ$.

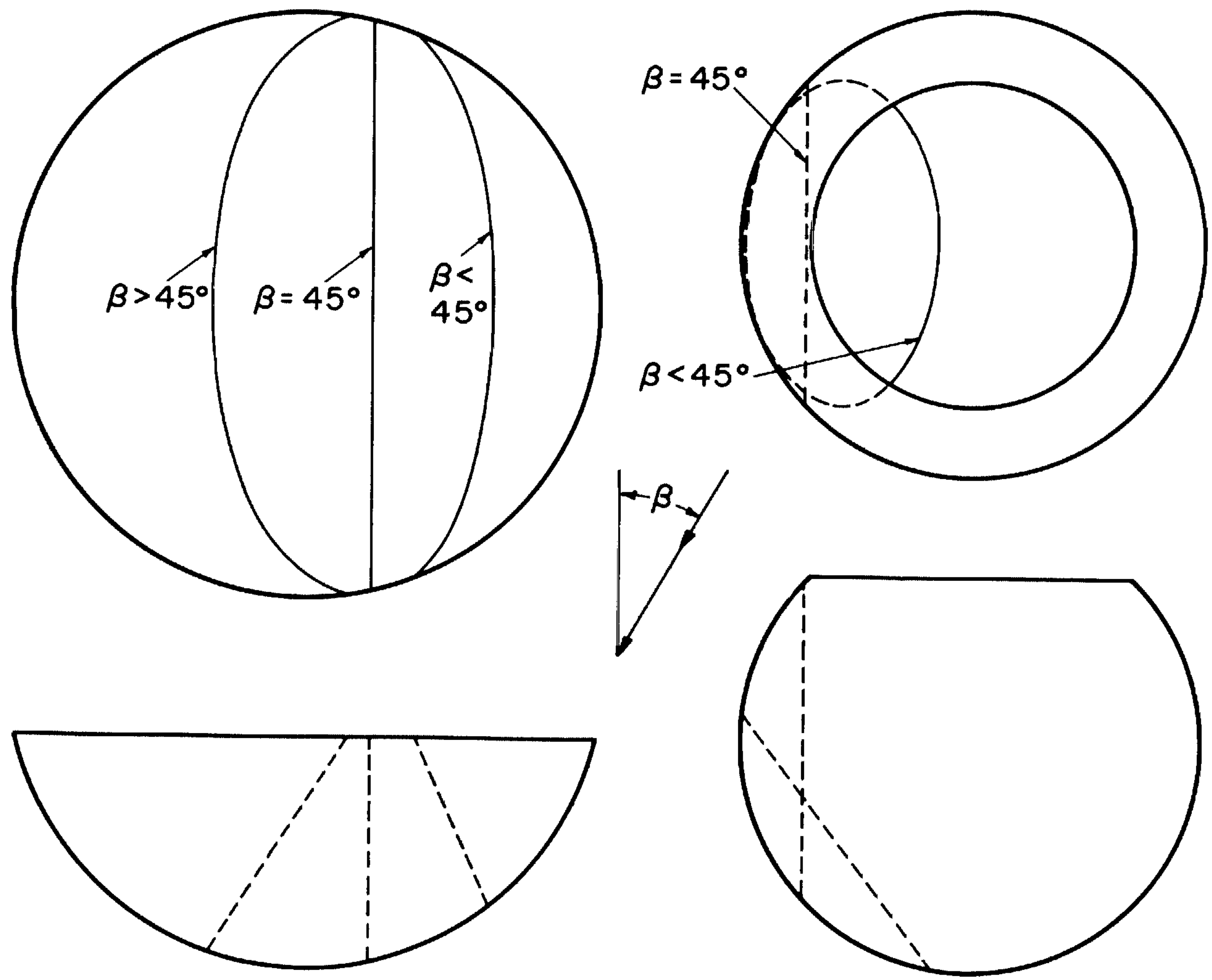

(a) Smaller than hemisphere; $\varphi^* > 90^\circ$.

(b) Larger than hemisphere; $\varphi^* < 90^\circ$.

Figure 4. - Projections of shadow, no-shadow boundary on plan and elevation views.

NASA TN D-1289
National Aeronautics and Space Administration.
ABSORPTION AND EMISSION CHARACTERISTICS OF DIFFUSE SPHERICAL ENCLOSURES. E. M. Sparrow and V. K. Jonsson, University of Minnesota. June 1962. 19p. OTS price, $0.50.
(NASA TECHNICAL NOTE D-1289)

An analysis was made to determine the energy absorbed when radiation from an external source enters a spherical cavity with diffusely reflecting walls. Both the over-all energy absorbed in the cavity and the local distribution of absorbed energy could be expressed in terms of simple algebraic equations valid for any arbitrary spatial and directional distribution of the incoming radiation. The characteristics of an isothermal spherical cavity as a possible source of near black-body radiation were also investigated, and this information was also expressed by simple algebraic relations.

I. Sparrow, Ephraim M.
II. Jonsson, V. K.
III. NASA TN D-1289

(Initial NASA distribution: 35, Power sources, supplementary; 36, Propellants; 43, Propulsion systems, other; 48, Space vehicles.)

NASA

NASA TN D-1289
National Aeronautics and Space Administration.
ABSORPTION AND EMISSION CHARACTERISTICS OF DIFFUSE SPHERICAL ENCLOSURES. E. M. Sparrow and V. K. Jonsson, University of Minnesota. June 1962. 19p. OTS price, $0.50.
(NASA TECHNICAL NOTE D-1289)

An analysis was made to determine the energy absorbed when radiation from an external source enters a spherical cavity with diffusely reflecting walls. Both the over-all energy absorbed in the cavity and the local distribution of absorbed energy could be expressed in terms of simple algebraic equations valid for any arbitrary spatial and directional distribution of the incoming radiation. The characteristics of an isothermal spherical cavity as a possible source of near black-body radiation were also investigated, and this information was also expressed by simple algebraic relations.

I. Sparrow, Ephraim M.
II. Jonsson, V. K.
III. NASA TN D-1289

(Initial NASA distribution: 35, Power sources, supplementary; 36, Propellants; 43, Propulsion systems, other; 48, Space vehicles.)

NASA

NASA TN D-1289
National Aeronautics and Space Administration.
ABSORPTION AND EMISSION CHARACTERISTICS OF DIFFUSE SPHERICAL ENCLOSURES. E. M. Sparrow and V. K. Jonsson, University of Minnesota. June 1962. 19p. OTS price, $0.50.
(NASA TECHNICAL NOTE D-1289)

An analysis was made to determine the energy absorbed when radiation from an external source enters a spherical cavity with diffusely reflecting walls. Both the over-all energy absorbed in the cavity and the local distribution of absorbed energy could be expressed in terms of simple algebraic equations valid for any arbitrary spatial and directional distribution of the incoming radiation. The characteristics of an isothermal spherical cavity as a possible source of near black-body radiation were also investigated, and this information was also expressed by simple algebraic relations.

I. Sparrow, Ephraim M.
II. Jonsson, V. K.
III. NASA TN D-1289

(Initial NASA distribution: 35, Power sources, supplementary; 36, Propellants; 43, Propulsion systems, other; 48, Space vehicles.)

NASA

NASA TN D-1289
National Aeronautics and Space Administration.
ABSORPTION AND EMISSION CHARACTERISTICS OF DIFFUSE SPHERICAL ENCLOSURES. E. M. Sparrow and V. K. Jonsson, University of Minnesota. June 1962. 19p. OTS price, $0.50.
(NASA TECHNICAL NOTE D-1289)

An analysis was made to determine the energy absorbed when radiation from an external source enters a spherical cavity with diffusely reflecting walls. Both the over-all energy absorbed in the cavity and the local distribution of absorbed energy could be expressed in terms of simple algebraic equations valid for any arbitrary spatial and directional distribution of the incoming radiation. The characteristics of an isothermal spherical cavity as a possible source of near black-body radiation were also investigated, and this information was also expressed by simple algebraic relations.

I. Sparrow, Ephraim M.
II. Jonsson, V. K.
III. NASA TN D-1289

(Initial NASA distribution: 35, Power sources, supplementary; 36, Propellants; 43, Propulsion systems, other; 48, Space vehicles.)

NASA